
Article:
Xie, Haiyan, Dawson, John F. orcid.org/0000-0003-4537-9977, Marvin, Andy C. orcid.org/0000-0003-2590-5335 et al. (1 more author) (2020) Numerical and theoretical analysis of stochastic electromagnetic fields coupling to a printed circuit board trace. IEEE Transactions on Electromagnetic Compatibility. pp. 1128-1135. ISSN 0018-9375

https://doi.org/10.1109/TEMC.2019.2954303

Numerical and Analytical Analysis of Stochastic Electromagnetic Fields Coupling to a Printed Circuit Board Trace

Haiyan Xie, *Member, IEEE*, John F. Dawson, *Member, IEEE*, Jiexiong Yan, Andy C. Marvin, *Fellow, IEEE*, and Martin P. Robinson, *Member, IEEE*

***Abstract*—Stochastic electromagnetic fields coupling to printed circuit board (PCB) traces are important to the understanding of electromagnetic compatibility at high frequencies when the circuits or systems are electrically large. In this article, it is studied both numerically and analytically, and the factors affecting the absorbed power are investigated. We present new methods to determine the level of coupling on PCB traces or other transmission lines on a dielectric substrate. A Monte Carlo method is applied to generate random uniform fields, and the quasi-TEM transmission line model is employed to compute the response of the trace for each plane wave numerically. In the analytical method, the closed-form expressions of the zero-order and the first-order approximations are established for the PCB trace. Based on the first-order approximation method and the numerical results, a computationally efficient empirical method is developed to estimate the power received. The absorbed power increases with frequency in the electrically short case after which multiple resonances can be seen. The absorbed power in the matched case is neither the largest nor the smallest among all the cases. It increases with the square of the substrate height but decreases with the permittivity of the substrate.**

***Index Terms*—Absorption cross section (ACS), printed circuit board (PCB) trace, stochastic electromagnetic fields, transmission-line coupling.**

I. Introduction

PRINTED circuit boards (PCBs) are an important factor in determining the electromagnetic compatibility of electronic systems. The absorption of electromagnetic power in the PCBs affects the overall immunity and (by reciprocity) the emissions of equipment. How the PCBs absorb electromagnetic power is important to study.

Manuscript received August 8, 2019; revised October 6, 2019 and October 31, 2019; accepted November 14, 2019. The work of H. Xie was supported by the China Scholarship Council. *(Corresponding author: Haiyan Xie.)*

H. Xie is with the Northwest Institute of Nuclear Technology, Shaanxi 710024, China, and also with the Department of Electronic Engineering, University of York, York YO10 5DD, U.K. (e-mail: xiehaiyan@nint.ac.cn).

J. F. Dawson, J. Yan, A. C. Marvin, and M. P. Robinson are with the Department of Electronic Engineering, University of York, York YO10 5DD, U.K. (e-mail: john.dawson@york.ac.uk; jy936@york.ac.uk; andy.marvin@york.ac.uk; martin.robinson@york.ac.uk).

Color versions of one or more of the figures in this article are available online at http://ieeexplore.ieee.org.

Digital Object Identifier 10.1109/TEMC.2019.2954303

Some research has been carried out to study the absorption cross section (ACS) of PCBs in reverberant (stochastic) environments. The average absorption cross sections (AACS) of different PCBs have been measured in a reverberation chamber from 2 to 20 GHz by Flintoft *et al.* [1], [2], where the PCBs with different component densities and surface shielding are considered. It was also found that the AACS of a PCB in the stack is reduced by 20%–40% compared with the value when the PCB isolated. The changes of a PCB's AACS due to the proximity to a reverberant chamber wall are studied in [3]. The result shows that the AACS can be reduced up to 30% when the PCB is placed parallel to the chamber wall with the components on the front of the PCB facing the wall. Based on the measured AACS data of PCBs and using the power balance concept, surrogates for real PCBs have been designed and calibrated for shielding measurements [4]. The results in [4] also show that the loads of the PCB trace play an important role in the AACS of PCB. However, what factors may affect the electromagnetic power absorbed by the loads of the PCB and how to predict the power quickly are not clear yet.

Stochastic electromagnetic fields coupling with transmission lines have been studied by some researchers. A semianalytical approach has been proposed by Junqua *et al*. [5] to evaluate the response of a wire in an electrically large cavity. Magdowski *et al.* [6] apply a numerical method to study the stochastic electromagnetic fields coupling to a transmission line in a reverberation chamber and obtain the average responses along the transmission line. They also developed a closed-form formula for the average response at the ends of the transmission line excited by the stochastic electromagnetic fields [7]. However, the results can not be used directly for the PCB trace because there is a substrate in the PCB. Veropoulos and Papakanellos [8] study twisted-wire pairs excited by random plane-wave fields. The same authors derive a closed-form expression for the probability density function of the induced far-end voltage of a PCB trace in certain cases of field descriptions [9]. In their study, the field amplitude and only one of the three angles, which are polarization angle, elevation angle of incidence, and azimuth angle of incidence, are random at the same time, while the other parameters of the field are fixed. This is different from the case of the stochastic fields in a reverberation chamber, where all the angles are random at the same time. Mehri *et al*. [10], [11]

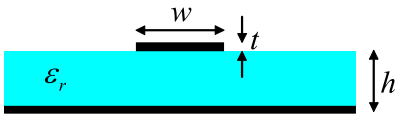

Fig. 1. Microstrip cross section of a PCB trace with height h, trace width w, and trace thickness t and relative permittivity ε_r of substrate.

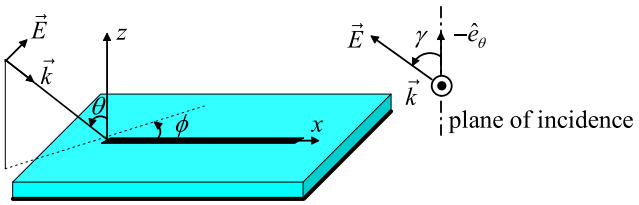

Fig. 2. Definitions of polar angle, azimuth angle, and polarization angle.

apply a trace orientation function, which is a function combining the trace location and its orientation, to statistically predict the PCB radiated susceptibility and emission. In their study, the trace orientation is random but the incident field is fixed that implies the elevation angle and the polarization angle are not random.

In this article, the problem of stochastic electric fields coupling to a PCB trace is studied numerically and analytically. Based on the analytic and numerical results, an empirical prediction method is developed to estimate the average voltage square and, thus, the power of the matched loads. Compared with the numerical method, the empirical method avoids large computation and can give quick estimates. The factors that affect the absorption of the electromagnetic power by the loads are investigated. Due to the influence of the dielectric on the excitation fields of the PCB trace, it is difficult to get a closed-form expression for the mean-squared voltage on the loads at the ends of a PCB trace if the loss of the trace is included, so the PCB trace is assumed to be lossless here. The study shows that the power absorbed by the load can be decreased by decreasing the PCB height and increasing the permittivity of the substrate.

In Section II, we introduce the numerical and analytical methods applied in this study. The terminal responses, the empirical method, and their distributions are given in Section III. The electromagnetic power absorbed by the loads and its change with the factors are presented in Section V, leading to the conclusions in Section VI.

II. Theoretical and Analytical Methods

A. Plane-Wave Field Coupling With PCB Trace

An analytical model for a plane-wave field coupling to a PCB trace, as shown in Fig. 1 and Fig. 2, has been derived by Leone and Singer [12]. This model is a quasi-TEM transmission-line model and the trace is described by its per-unit length transmission-line parameters. The voltages at the ends of the trace are given by

$$\begin{pmatrix} V_0 \\ V_L \end{pmatrix} = \frac{1}{e^{j2\beta L} - \rho_0\rho_L} \begin{bmatrix} (1+\rho_0)\left(\rho_L S_1 + e^{j\beta L} S_2\right) \\ (1+\rho_L)\left(e^{j\beta L} S_1 + \rho_0 S_2\right) \end{bmatrix} \quad (1)$$

where V_0 and V_L are the voltages at the near and far ends, respectively. ρ_0 and ρ_L are the reflection coefficients at the ends and are defined by

$$\rho_{0,L} = \frac{Z_{0,L} - Z_C}{Z_{0,L} + Z_C} \quad (2)$$

with the terminal loads Z_0, Z_L, and the characteristic impedance Z_C, which is computed empirically using the approximations given in [12].

β is the propagation constant and is given by

$$\beta = k_0\sqrt{\varepsilon_{r,\text{eff}}} \quad (3)$$

with $k_0 = \omega\sqrt{\mu_0\varepsilon_0}$ is the free-space wave number and $\varepsilon_{r,\text{eff}}$ is the effective relative permittivity computed as in [12]. L is the trace length. Under the assumption that the height h of the PCB substrate is much smaller than the substrate wavelength, the sources S_1 and S_2 can be approximated by

$$S_{1,2} \approx \pm jk_0 hE_i e^{-j\alpha} e^{j\beta x_{1,2}} \frac{e^{j(\pm\beta - k_x)L} - 1}{j\left(\pm\beta - k_x\right)} \cdot \left(\sin\phi\sin\gamma\cos\theta + \cos\phi\cos\gamma \mp \frac{\sqrt{\varepsilon_{r,\text{eff}}}}{\varepsilon_r}\sin\theta\cos\gamma\right). \quad (4)$$

Here θ and ϕ are the polar angle and azimuth angle of the incidence, respectively. γ is the polarization angle of the incident field, as shown in Fig. 2. $k_x = k_0\sin\theta\cos\phi$ is the x component of wave vector $\mathbf{k}_0$. E_i is the electric magnitude of the plane-wave field. α is the phase angle of an electric field, which is added to the (4) to account for the influence of the electric field's phase angle. $x_1 = 0$ and $x_2 = L$ are the x coordinates of the near and far ends of trace, respectively.

B. Analytical Methods for Stochastic Excitation

The squared magnitude of the voltage is an important parameter because it is proportional to the power absorbed by the loads. According to (1), the square magnitude of the voltage is given by

$$|V_0|^2 = \frac{|1+\rho_0|^2}{\left|e^{j2\beta L} - \rho_0\rho_L\right|^2}\left|\rho_L S_1 + e^{j\beta L} S_2\right|^2 \quad (5)$$

$$|V_L|^2 = \frac{|1+\rho_L|^2}{\left|e^{j2\beta L} - \rho_0\rho_L\right|^2}\left|e^{j\beta L} S_1 + \rho_0 S_2\right|^2. \quad (6)$$

The mean-square magnitude of the voltage at the end of the PCB trace excited by the stochastic electromagnetic fields inside a reverberation chamber is given by

$$\left\langle |V_{0,L}|^2 \right\rangle = \frac{1}{2\pi}\int_0^{2\pi}\frac{1}{2}\int_0^{\pi/2}\frac{1}{\pi}\int_0^{\pi}\frac{1}{2\pi}\int_0^{2\pi}|V_{0,L}|^2 \times \sin\theta\, d\alpha\, d\gamma\, d\theta\, d\phi. \quad (7)$$

Here $\langle\ \rangle$ denotes the average over all the incident angles, the polarization angle, and the phase angle. The polar angle $\theta \in [0, \pi/2]$ in (7), because only the plane wave from the upper hemisphere can couple to the PCB trace. However, it is impossible to get the closed-form expression for $\langle |V_{0,L}|^2 \rangle$ directly, because the expressions of S_1 and S_2 in (4) are very complicated. In order to derive a closed-form expression, some assumptions can be made.

1) Low-Frequency Approximation (Zero Order): Under the low-frequency approximation $|\mp\beta - k_x|L \ll 1$, according to (4), $S_{1,2}$ can be written as

$$S_{1,2} \approx \pm jk_0 hLE_i e^{-j\alpha} e^{j\beta x_{1,2}} \cdot \left(\sin\phi\sin\gamma\cos\theta + \cos\phi\cos\gamma \mp \frac{\sqrt{\varepsilon_{r,\text{eff}}}}{\varepsilon_r}\sin\theta\cos\gamma\right). \tag{8}$$

Then, according to (1), the voltages are given by

$$V_0 = \frac{jk_0 hLE_i e^{-j\alpha} e^{j\beta x_1}(1+\rho_0)}{e^{j2\beta L} - \rho_0\rho_L} \times \left[\left(\rho_L - e^{2j\beta L}\right)\cdot(\sin\phi\sin\gamma\cos\theta + \cos\phi\cos\gamma) + \left(\rho_L + e^{2j\beta L}\right)\frac{\sqrt{\varepsilon_{r,\text{eff}}}}{\varepsilon_r}\sin\theta\cos\gamma\right] \tag{9}$$

$$V_L = \frac{jk_0 hLE_i e^{-j\alpha} e^{j\beta x_2}(1+\rho_L)}{e^{j2\beta L} - \rho_0\rho_L} \times \left[(1-\rho_0)\cdot(\sin\phi\sin\gamma\cos\theta + \cos\phi\cos\gamma) + (1+\rho_0)\frac{\sqrt{\varepsilon_{r,\text{eff}}}}{\varepsilon_r}\sin\theta\cos\gamma\right]. \tag{10}$$

With the definition of the average operator $\langle\ \rangle$, we can obtain

$$\langle V_0\rangle = \langle V_L\rangle = 0 \tag{11}$$

directly. According to the Appendix, the mean-square magnitude of the voltage is given by

$$\left\langle |V_0|^2 \right\rangle = \frac{(k_0 hLE_i)^2}{6}\frac{|1+\rho_0|^2}{|e^{j2\beta L} - \rho_0\rho_L|^2} \cdot \left[\left|1 - \rho_L e^{-2j\beta L}\right|^2 + \frac{\varepsilon_{r,\text{eff}}}{\varepsilon_r^2}\left|1 + \rho_L e^{-2j\beta L}\right|^2\right] \tag{12}$$

$$\left\langle |V_L|^2 \right\rangle = \frac{(k_0 hLE_i)^2}{6}\frac{|1+\rho_L|^2}{|e^{j2\beta L} - \rho_0\rho_L|^2} \cdot \left[|1-\rho_0|^2 + \frac{\varepsilon_{r,\text{eff}}}{\varepsilon_r^2}|1+\rho_0|^2\right]. \tag{13}$$

Then the average power absorbed by the loads can be written as

$$\langle P_{0,L}\rangle = \left\langle |V_{0,L}|^2 \right\rangle \text{Re}\left(\frac{1}{{Z_{0,L}}^*}\right). \tag{14}$$

TABLE I
STATISTICAL DISTRIBUTION OF ANGLES

Name	Distribution
azimuth angle ϕ	U(0,2π)
polar angle θ	arccos(U(0,1))
phase angle α	U(0,2π)
angle of polarization γ	U(0,π)

2) Low-Frequency Approximation (First Order): For the PCB trace with matched loads, the first-order approximation is used due to better accuracy. When the ends are matched, ρ_0 and ρ_L in (5) and (6) equals 0, and then the voltage magnitude squares are given by

$$|V_0|^2 = |S_2|^2 \tag{15}$$

$$|V_L|^2 = |S_1|^2. \tag{16}$$

The term in (4) can be written as

$$\frac{e^{j(\pm\beta - k_x)L} - 1}{j(\pm\beta - k_x)} = L\sin c\left(\frac{(\pm\beta - k_x)L}{2}\right)e^{j\frac{(\pm\beta - k_x)L}{2}}. \tag{17}$$

The function $\sin cx$ in (17) can be approximated by

$$\sin cx \approx 1 - x^2/6. \tag{18}$$

Substituting (17) into (4) and then into (15) and (16), and with the average operation, the mean-square magnitude of the voltage can be approximated by (19), more details can be found in the Appendix.

$$\left\langle |V_{0,L}|^2 \right\rangle \approx \frac{4}{35}(hE_i)^2\xi\left\{\left[\left(1 + \frac{\varepsilon_{r,\text{eff}}}{\varepsilon_r^2}\right)\cdot\left(35\varepsilon_{r,\text{eff}}^2 + 84\varepsilon_{r,\text{eff}} + 9\right) + 140\frac{\varepsilon_{r,\text{eff}}^2}{\varepsilon_r} + 84\frac{\varepsilon_{r,\text{eff}}}{\varepsilon_r}\right]\xi^2 - \left[\left(1 + \frac{\varepsilon_{r,\text{eff}}}{\varepsilon_r^2}\right)(70\varepsilon_{r,\text{eff}} + 28) + 140\frac{\varepsilon_{r,\text{eff}}}{\varepsilon_r}\right]\xi + 35\left(1 + \frac{\varepsilon_{r,\text{eff}}}{\varepsilon_r^2}\right)\right\} \tag{19}$$

with

$$\xi = k_0^2 L^2/24. \tag{20}$$

C. Numerical Method Based on Monte Carlo (MC) Method

In the high-frequency range, it is difficult to get a closed form for the average value directly. A numerical method is needed to get the results. Hill [14] proposed that the stochastic field inside a reverberation chamber could be represented by a plane-wave integral. Instead of an integral, we employ a finite number *N* of plane waves in the numerical simulation for each boundary condition. The MC method is applied to generate a set of plane waves with finite number *N* [6], [15]. For *B* different boundary conditions with each having *N* plane waves are generated. In the numerical method, the angles ϕ, γ, and α are equally distributed between [0, 2π], [0, π], and [0, 2π], respectively, as shown in Table I. In order to discard the sinθ from the summand [6] and

only considering the plane wave from the upper hemisphere, the polar angle θ must be statistically distributed according to arccos(U(0, 1)), where U(0, 1) is a uniform distribution between [0, 1].

For each plane wave, the coupled voltage is computed by using (1) and replacing E_i in (4) with E_N, where E_N is the electric magnitude of each plane wave. The electric magnitude E_N should obey the following normalization rule:

$$E_N = \frac{E_0}{\sqrt{2N}}. \tag{21}$$

Here, E_0 is the mean magnitude of the total field in the reverberation chamber. It has a simple relation with the magnitude in the theoretical method, $E_0 = E_i$.

D. Gauss–Legendre Quadrature (GLQ) Combined With Full-Wave Simulation

For the sake of comparison, the results are also evaluated numerically using GLQ on a sphere [4], [16]. The voltage magnitude square can be approximated by

$$\left\langle |V|^2 \right\rangle = \frac{1}{8L_P} \sum_{l=1}^{L_P} \sum_{m=1}^{2L_P} \omega_l \times \left(\left| V^{\mathrm{TE}}(\theta_l, \phi_m) \right|^2 + \left| V^{\mathrm{TM}}(\theta_l, \phi_m) \right|^2 \right). \tag{22}$$

Here L_P is the order of the Legendre polynomial. The azimuth angle ϕ_m is sampled at $\phi_m = m\pi/L$ ($m = 1, \ldots, 2L$) and the polar angle θ_L corresponding to the zeros of the Legendre polynomial of order L_P, $P_L(\cos(\theta)) = 0$. ω_l is the Gauss–Legendre weighting factor. V^{TE} and V^{TM} represent the voltages generated by the transverse electric and transverse magnetic polarized waves, respectively. The order L_P must satisfy [4]

$$L_P \geq \pi + 10D f_{\max}^{\mathrm{GHz}} \tag{23}$$

where D is the maximum linear size of an object and $f_{\max}^{\mathrm{GHz}}$ is the desired maximum frequency in gigahertz.

The full-wave simulator, CST microwave studio [17], is employed to compute the voltage of the trace load under the plane-wave illumination by TE and TM polarized waves from spherical direction (θ_l, ϕ_l).

III. Comparison Between Different Methods

The length of the trace is 80 mm. The height h of the trace over the ground is 0.8 mm. The characteristic impedance of the trace is 50 Ω. The chamber constant E_0 is set to 1. In the numerical method based on MC, N and B are set to 100 and 500, respectively. The mean-square magnitude of the voltage is computed by using the numerical method and the theoretical method.

Fig. 3 shows the mean-square magnitude of the voltage obtained by the numerical method, zero-order approximation, and first-order approximation, when the PCB trace is matched at both ends and the substrate is made of FR4, where the relative permittivity is set to $\varepsilon_r = 4.4$ and, thus, $\varepsilon_{r,\mathrm{eff}} = 3.3149$.

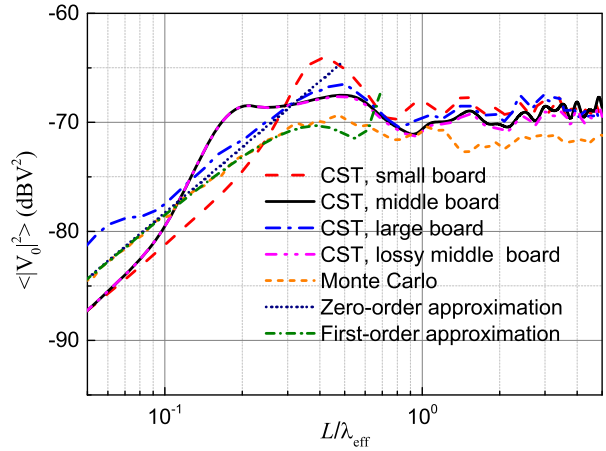

Fig. 3. Mean-square magnitude of the voltage obtained by different methods for FR4 substrate when $Z_0 = Z_L = Z_C = 50\ \Omega$ and $h = 0.8$ mm.

In the figure, λ_{eff} is the effective wavelength in the PCB and is given by

$$\lambda_{\mathrm{eff}} = \lambda_0 / \sqrt{\varepsilon_{r,\mathrm{eff}}} \tag{24}$$

where λ_0 is the wavelength in the free space. The result shows that the zero-order approximation, i.e., (12) and (13), can give good prediction up to $L/\lambda_{\mathrm{eff}} = 0.2$, while the first-order approximation, i.e., (19), can give good prediction up to $L/\lambda_{\mathrm{eff}} = 0.4$, when the mean-square magnitude of the voltage reaches the maximum. The results from GLQ combined with the full-wave simulation in Section II-D, denoted by "CST" in the figure, are also given. According to (23), the value of L_P is large and it is too high for a practical simulation with CST. We found that the order of 4, e.g., 64 plane waves in total, was sufficient to achieve good accuracy for this problem. While the PCB is infinite in the analytical and MC methods, it is finite in the CST simulation. To show the influence of the board size, a small board (100 mm × 60 mm), a middle-sized board (140 mm × 100 mm), and a large board (1000 mm × 800 mm) are computed. It can be seen that the larger the board, the better the "CST" result approaches the results of the numerical method based on MC described in Section II-C, which is denoted by "MC" in the figure. In the high-frequency range, the CST results are 2 dB larger than the MC result; however, in the low-frequency range, the former is about 2 dB less than the latter. For the small PCB, the difference can be up to 6 dB at $L/\lambda_{\mathrm{eff}} = 0.4$. To show the loss effect, the "CST" result of the lossy middle board is also given, where the loss tangent of FR4 and the copper conductivity are set to 0.01 and 5.7×10^7 S/m, respectively. However, the difference between the lossless and lossy "CST" results is less than 1.5 dB, when L/λ_{eff} is up to 5.

Fig. 4 shows the mean-square magnitude of the voltages obtained by the numerical method based on the MC and theoretical method for different substrates, whose relative permittivity is given in Table II. The trace width w and thickness t are adjusted to keep the characteristic impedance Z_C and height h the same for different substrates in the simulation. The results show that (19) can be employed to predict the mean-square magnitude of

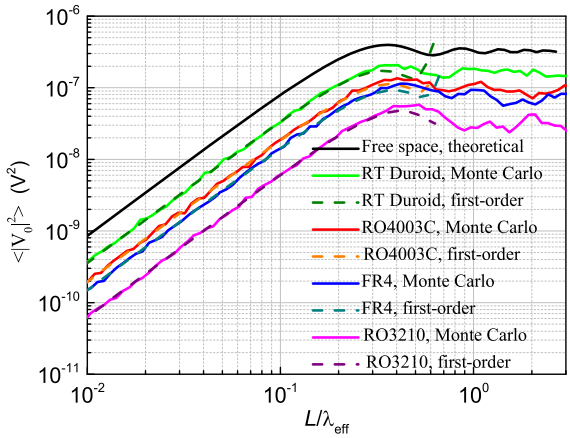

Fig. 4. Mean-square magnitude of the voltage obtained by the numerical method and the first-order approximation for different substrates when $Z_0 = Z_L = Z_C = 50\ \Omega$ and $h = 0.8$ mm.

TABLE II
RELATIVE PERMITTIVITY OF SUBSTRATE

Type	Relative permittivity ε_r
FR4	4.4
RT Duroid	1.96
RO3210	10.8
RO4003C	3.38

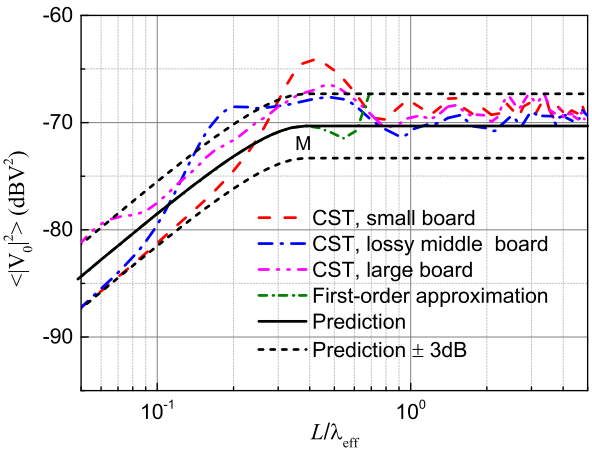

Fig. 5. Prediction result of PCB with FR4 substrate when $Z_0 = Z_L = Z_C = 50\ \Omega$ and $h = 0.8$ mm.

the voltage up to the first maximum, even for the other kinds of substrates.

IV. EMPIRICAL PREDICTION METHOD

Based on the first-order approximation and the numerical results, an empirical method can be developed to estimate the average voltage square and, thus, the power very quickly. The first maximum point "M" is found first in the first-order approximation curve, as shown in Fig. 5, and then a new curve "Prediction" is plotted shown as the black solid curve in Fig. 5, whose value in the high-frequency range equals the point "M."

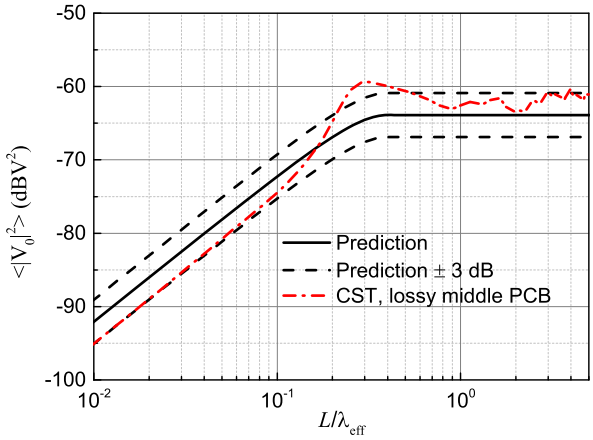

Fig. 6. Prediction result of another PCB with FR4 substrate when $h = 1.55$ mm, $w = 0.48$ mm, $t = 18\ \mu$m, and $Z_0 = Z_L = Z_C = 115\ \Omega$.

The actual voltage square is nearly in the range of "Prediction ±3 dB" shown as the black dotted curves in Fig. 5.

Fig. 6 shows the prediction of another PCB with FR4 dielectric compared with the "CST" result of a middle-size PCB, where $h = 1.55$ mm, $w = 0.48$ mm, $t = 18\ \mu$m, $Z_0 = Z_L = Z_C = 115\ \Omega$, and $\varepsilon_{r,\text{eff}} = 2.9669$. The results show that the average voltage magnitude square $<|V_0|^2>$ obtained by GLQ combined with the CST simulation is nearly in the range of the "Prediction ±3 dB."

V. POWER ABSORBED AND INFLUENCING FACTORS

In order to study the factors that are important for the absorbed power, the power absorbed by the loads is computed by using the numerical method based on MC when the PCB trace has different lengths, loads, heights, and substrates. In the study, the width w and the thickness t of the PCB trace are adjusted to keep the characteristic impedance $Z_C = 50\ \Omega$ in all the cases.

A. Influence of Trace Length

The square magnitude of the voltage changing with L/λ_{eff} is shown in Figs. 3 and 4. The absorbed power is proportional to the square magnitude of the voltage. Thus, the power has the same trend. The results show that the power increases with the trace length in the low-frequency range. This can also be concluded from (19) that $P \propto (hL)^2$ in the low-frequency range. It implies that the absorbed power is proportional to the area square of the loop which is made up of the trace, the loads, and the ground. The absorbed power will oscillate with L/λ_{eff} a little after it reaches the maximum. Fig. 7 shows the total power absorbed at the loads obtained by the numerical method based on MC when the PCB trace is 60, 80, 100, and 120 mm long with the matched loads, FR4 substrate, and the height of 0.8 mm. The results show that the trace length does not change the maximum of the absorbed power, which can also be predicted by (19). Because the power is a function of $\xi = k_0^2 L^2/24$, the value of maximum does not change with the trace length L but shifts in the frequency with it. As a result, the curve moves toward the left when the trace length becomes large in the low-frequency range.

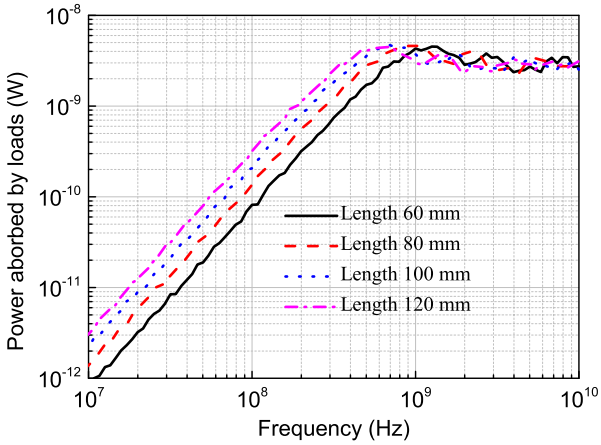

Fig. 7. Total power absorbed at the loads obtained by the numerical method based on MC when the PCB trace is matched at both ends and has different trace lengths, with FR4 substrate and height of 0.8 mm.

B. *Influence of Terminal Loads*

Fig. 8 shows the power absorbed by the loads when the loads have different values. The near end is matched and the far end has different values. The PCB trace is 80 mm long with 0.8 mm FR4 substrate. When $Z_L = Z_C$, the power absorbed by Z_L is the largest in all the cases; however, the power absorbed by Z_0 is not the largest. The total power absorbed by the two ends when they are matched is neither the largest nor the smallest in all the cases. When considering the power absorbed by the load Z_L, we can consider the port of the load Z_L as the port of an antenna, which is made of the trace, the ground, and the load Z_0. The input power of the port is unchanged due to $Z_0 = Z_C$ in all cases, and then the input power will be absorbed by Z_L totally when $Z_L = Z_C$. This is the reason why the power absorbed by Z_L is largest when $Z_L = Z_C$. However, when we look at the port of Z_0 and considering the rest as an antenna, the antenna is different for different Z_L and changes with the frequency. But in the low-frequency range, the trace with the loads can be considered as a voltage divider, comprising Z_0 and Z_L. Thus, the power of Z_0 nearly decreases with Z_L at the low frequencies.

The power absorbed by Z_0 when $Z_L = 1/100Z_C$, $1/10Z_C$, or $1/2Z_C$ is different from that when $Z_L = 100Z_C$, $10Z_C$, or $2Z_C$, respectively, which is different from the case of the transmission line in free space [3]. This can also be concluded from (12). $\langle |V_0|^2 \rangle$ changes if ρ_L is replaced by -ρ_L when the relative permittivity $\varepsilon_r \neq 1$ in the case $\rho_0 = 0$; however, it does not change when the relative permittivity $\varepsilon_r = 1$.

The measurement by Flintoft *et al.* [1] shows that the ACS of PCB is stable in the high-frequency range, not like the oscillation in Figs. 7 and 8. This is because there are many traces with different lengths and loads on a real PCB. The power absorbed via every trace has oscillations at the high frequency, but the powers for the different traces have oscillations at different frequencies. As a result, the overall ACS is generally stable in the high-frequency range. Fig. 9 shows the sum of the powers absorbed by four PCB traces and it is more stable than the single one.

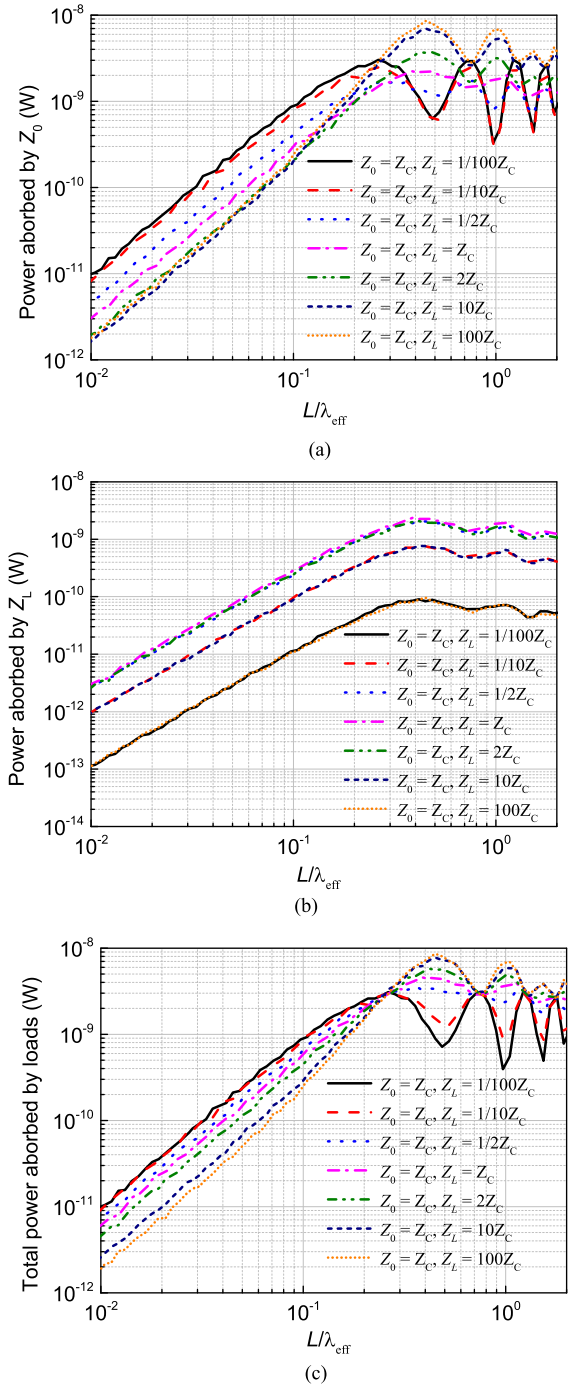

Fig. 8. Power absorbed by the loads when the PCB trace has different loads, with FR4 substrate and the height of 0.8 mm. (a) Power absorbed by Z_0. (b) Power absorbed by Z_L. (*c*) Total power.

C. *Influence of PCB Height*

Fig. 10 shows the absorbed power when the PCB has different heights with the same characteristic impedance $Z_c = 50\,\Omega$, where the trace length is 80 mm and is matched at both ends. The substrate is made of FR4. The results show that the height greatly affects the power absorbed by the loads. The power generally increases with h^2, also predicted by (19), in the case when a quasi-TEM transmission-line model for the PCB trace is valid.

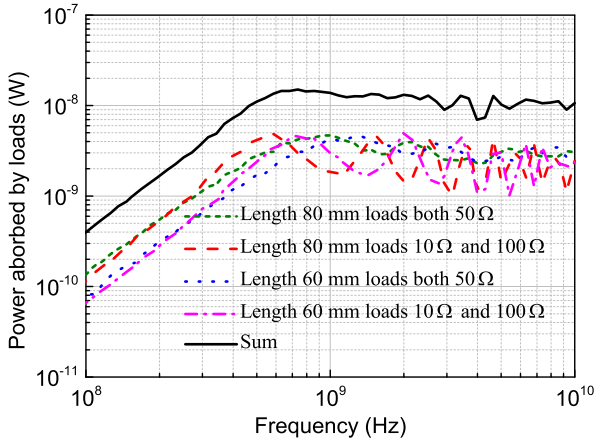

Fig. 9. Sum of the powers absorbed via four traces, with 0.8 mm FR4 substrate and characteristic impedance 50 Ω.

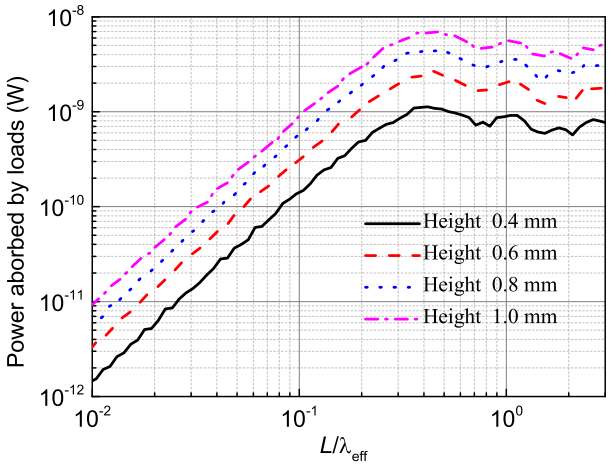

Fig. 10. Total power absorbed by the loads when the PCB trace is matched at both ends and has different heights, with FR4 substrate and trace length of 0.8 mm.

D. Influence of Different Substrate

The influence of different substrates should be investigated. Four kinds of substrates, FR4, RT Duroid, RO4003, and RO3210, are considered and their relative permittivity is given in Table II. For the sake of comparison, the result of a single line over an infinite and perfectly conducting ground without the substrate is given too, as shown in Figs. 4 and 11. In all the cases, the characteristic impedance $Z_C = 50\ \Omega$, the height $h = 0.8$ mm, and the length $L = 80$ mm.

The results show that the larger the permittivity, the lower will be the frequency where the power reaches the maximum. If the curve is plotted versus L/λ_{eff}, as shown in Fig. 4, however, the maximum happens at the larger value of L/λ_{eff} for substrate with larger permittivity. The results also show that the larger the relative permittivity, the less power will be absorbed by the PCB trace. This can be due to that the larger the permittivity of the substrate the more power of the electromagnetic field will be reflected by the substrate.

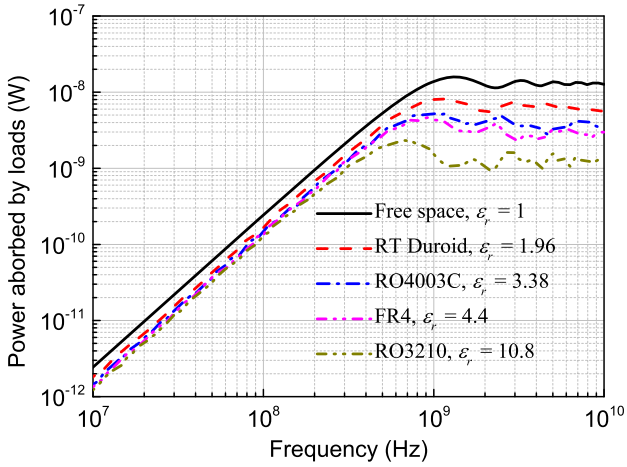

Fig. 11. Total power absorbed by the loads when the PCB trace is matched at both ends and has different substrates, with a height of 0.8 mm and a trace length of 0.8 mm.

VI. Conclusion

Stochastic fields inside a reverberation chamber coupling to PCB traces have been studied numerically and theoretically. In the numerical method, an MC method is applied to generate the random uniform fields inside a reverberation chamber, and the quasi-TEM transmission line model is employed to compute the response of the trace for each plane wave. In the theoretical method, the closed-form expressions of the zero-order and first-order approximations are established for the unmatched and matched PCB trace, respectively. The numerical method, where the PCB is infinite, is verified by the full-wave simulation, where the PCB is finite. Based on the first-order approximation and the numerical results, an empirical method is developed to predict the average voltage square and, thus, power of the matched loads. Compared with the numerical method and full-wave simulation, the empirical method avoids large computation and can provide quick results for the designers.

The influences of the trace length, the trace height, the terminal loads, and the relative permittivity of the substrate on the power absorbed by the loads are studied. The length does not affect the maximum power. The absorbed power for the matched case is neither the largest nor the smallest in all the cases. The absorbed power can be affected by the substrate height greatly. It is proportional to h^2 when the quasi-TEM transmission-line model is valid. The PCB trace with the substrate of larger permittivity will absorb less electromagnetic power.

In the future, we will study the power absorbed by the substrate and compare it with that absorbed by the PCB trace.

Appendix

According to (1), the square magnitude of voltage V_0 can be written as

$$|V_0|^2 = \frac{|1+\rho_0|^2}{|e^{j2\beta L} - \rho_0\rho_L|^2}\left[|\rho_L|^2|S_1|^2 + \rho_L e^{-j\beta L}S_1S_2^* + \rho_L^* e^{j\beta L}S_1^2S_2 + |S_2|^2\right]. \quad (25)$$

Then, the mean-square magnitude is given by

$$\left\langle |V_0|^2 \right\rangle = \frac{|1+\rho_0|^2}{|e^{j2\beta L} - \rho_0\rho_L|^2} \Big[|\rho_L|^2 \left\langle |S_1|^2 \right\rangle + \rho_L e^{-j\beta L} \langle S_1 S_2^* \rangle + \rho_L^* e^{j\beta L} \left\langle S_1^2 S_2 \right\rangle + \left\langle |S_2|^2 \right\rangle \Big]. \tag{26}$$

Under the low-frequency approximation (8)

$$\left\langle |S_{1,2}|^2 \right\rangle \approx \frac{(k_0 h L E_i)^2}{6} \left(1 + \frac{\varepsilon_{r,\text{eff}}}{\varepsilon_r^2} \right) \tag{27}$$

$$\langle S_1 S_2^* \rangle \approx -\frac{1}{6} \left(1 - \frac{\varepsilon_{r,\text{eff}}}{\varepsilon_r^2} \right) (k_0 h L E_i)^2 e^{-j\beta L}. \tag{28}$$

Substituting (27) and (28) into (25) gives (12). Equation (13) can be obtained in a similar way.

If the PCB trace is matched, the square magnitude of voltage is given by (15) and (16). Using the first-order approximation (18), the square magnitude of the voltage can be written as

$$|V_{0,L}|^2 \approx (k_0 h L E_i)^2 \left[A + B \sin^2\theta \cos^2\phi + C \sin\theta \cos\phi \right]^2 \cdot (\sin\phi \sin\gamma \cos\theta + \cos\phi \cos\gamma + D \sin\theta \cos\gamma)^2 \tag{29}$$

where

$$A = \left(1 - \frac{k_0^2 L^2}{24} \varepsilon_{r,\text{eff}} \right) \tag{30}$$

$$B = -\frac{k_0^2 L^2}{24} \tag{31}$$

$$C = \mp \frac{k_0^2 L^2 \sqrt{\varepsilon_{r,\text{eff}}}}{12} \tag{32}$$

$$D = \pm \frac{\sqrt{\varepsilon_{r,\text{eff}}}}{\varepsilon_r}. \tag{33}$$

According to the definition of the average (7), the mean-square magnitude of the voltage is given by

$$\left\langle |V_{0,L}|^2 \right\rangle = (k_0 h L E_i)^2 \left[(1+D^2) \left(\frac{A^2}{6} + \frac{3}{70} B^2 + \frac{1}{15} C^2 + \frac{2}{15} AB \right) + \frac{ACD}{3} + \frac{1}{5} BCD \right]. \tag{34}$$

Substituting (30)–(33) into (34) gives (19).

REFERENCES

[1] I. D. Flintoft, S. J. Bale, S. L. Parker, A. C. Marvin, J. F. Dawson, and M. P. Robinson, "Measured average absorption cross-sections of printed circuit boards from 2 to 20 GHz," *IEEE Trans. Electromagn. Compat.*, vol. 58, no. 2, pp. 553–560, Apr. 2016.

[2] S. L. Parker *et al.*, "Absorption cross section measurement of stacked PCBs in a reverberation chamber," in *Proc. Asia-Pac. Int. Symp. Electromagn. Compat.*, 2016, pp. 991–993.

[3] S. L. Parker *et al.*, "Changes in a printed circuit board's absorption cross section due to proximity to walls in a reverberant environment," in *Proc. IEEE Int. Symp. Electromagn. Compat.*, 2016, pp. 818–823.

[4] I. D. Flintoft *et al.*, "Representative contents design for shielding enclosure qualification from 2 to 20 GHz," *IEEE Trans. Electromagn. Compat.*, vol. 60, no. 1, pp. 173–181, Feb. 2018.

[5] I. Junqua, J.-P. Parmantier, and P. Degauque, "Field-to-wire coupling in an electrically large cavity: A semianalytic solution," *IEEE Trans. Electromagn. Compat.*, vol. 52, no. 4, pp. 1034–1040, Nov. 2010.

[6] M. Magdowski, S. V. Tkachenko, and R. Vick, "Coupling of stochastic electromagnetic fields to a transmission line in a reverberation chamber," *IEEE Trans. Electromagn. Compat.*, vol. 53, no. 2, pp. 308–317, May 2011.

[7] M. Magdowski and R. Vick, "Closed-form formulas for the stochastic electromagnetic field coupling to a transmission line with arbitrary loads," *IEEE Trans. Electromagn. Compat.*, vol. 54, no. 5, pp. 1147–1152, Oct. 2012.

[8] G. P. Veropoulos and P. J. Papakanellos, "A probabilistic approach for the susceptibility assessment of twisted-wire pairs excited by random plane-wave fields," *IEEE Trans. Electromagn. Compat.*, vol. 59, no. 3, pp. 962–969, Jun. 2017.

[9] G. P. Veropoulos, P. J. Papakanellos, and C. Vlachos, "A probabilistic approach for the susceptibility assessment of a straight PCB trace excited by random plane-wave fields," *IEEE Trans. Electromagn. Compat.*, vol. 60, no. 1, pp. 258–265, Feb. 2018.

[10] M. Mehri, N. Masoumi, and J. Rashed-Mohassel, "Trace orientation function for statistical prediction of PCB radiated susceptibility and emission," *IEEE Trans. Electromagn. Compat.*, vol. 57, no. 5, pp. 1168–1178, Oct. 2015.

[11] M. Mehri and N. Masoumi, "Statistical prediction and quantification of radiated susceptibility for electronic systems PCB in electromagnetic polluted environments," *IEEE Trans. Electromagn. Compat.*, vol. 59, no. 2, pp. 498–508, Apr. 2017.

[12] M. Leone and H. L. Singer, "On the coupling of an external electromagnetic field to a printed circuit board trace," *IEEE Trans. Electromagn. Compat.*, vol. 41, no. 4, pp. 418–424, Nov. 1999.

[13] K. C. Gupta, R. Garg, and R. Chada, *Computer-Aided Design of Microwave Circuits*. Norwood, MA, USA: Artech House, 1981.

[14] D. A. Hill, "Plane wave integral representation for fields in reverberation chambers," *IEEE Trans. Electromagn. Compat.*, vol. 40, no. 3, pp. 209–217, Aug. 1998.

[15] L. Musso, V. Berat, F. Canavero, and B. Demoulin, "A plane wave Monte Carlo simulation method for reverberation chambers," in *Proc. Int. Symp. Electromagn. Compat.*, 2002, pp. 1–6.

[16] K. Atkinson, "Numerical integration on the sphere," *J. Aust. Math. Soc., B*, vol. 23, pp. 332–347, 1982.

[17] Microwave Studio, Computer Simulation Technology, 2015. [Online]. Available: https://www.cst.com